Get Clarity On Generics
Cost-Effective CT & MRI Contrast Agents
FRESENIUS KABI
WATCH VIDEO

AJNR

This information is current as of August 4, 2025.

Reconstruction of the Corticospinal Tract in Patients with Motor-Eloquent High-Grade Gliomas Using Multilevel Fiber Tractography Combined with Functional Motor Cortex Mapping

A. Zhylka, N. Sollmann, F. Kofler, A. Radwan, A. De Luca, J. Gempt, B. Wiestler, B. Menze, A. Schroeder, C. Zimmer, J.S. Kirschke, S. Sunaert, A. Leemans, S.M. Krieg and J. Pluim

AJNR Am J Neuroradiol published online 16 February 2023
http://www.ajnr.org/content/early/2023/02/16/ajnr.A7793

Published February 16, 2023 as 10.3174/ajnr.A7793

Reconstruction of the Corticospinal Tract in Patients with Motor-Eloquent High-Grade Gliomas Using Multilevel Fiber Tractography Combined with Functional Motor Cortex Mapping

A. Zhylka, N. Sollmann, F. Kofler, A. Radwan, A. De Luca, J. Gempt, B. Wiestler, B. Menze, A. Schroeder, C. Zimmer, J.S. Kirschke, S. Sunaert, A. Leemans, S.M. Krieg, and J. Pluim

ABSTRACT

BACKGROUND AND PURPOSE: Tractography of the corticospinal tract is paramount to presurgical planning and guidance of intraoperative resection in patients with motor-eloquent gliomas. It is well-known that DTI-based tractography as the most frequently used technique has relevant shortcomings, particularly for resolving complex fiber architecture. The purpose of this study was to evaluate multilevel fiber tractography combined with functional motor cortex mapping in comparison with conventional deterministic tractography algorithms.

MATERIALS AND METHODS: Thirty-one patients (mean age, 61.5 [SD, 12.2] years) with motor-eloquent high-grade gliomas underwent MR imaging with DWI (TR/TE = 5000/78 ms, voxel size = 2 × 2 × 2 mm^3, 1 volume at b = 0 s/mm^2, 32 volumes at b = 1000 s/mm^2). DTI, constrained spherical deconvolution, and multilevel fiber tractography–based reconstruction of the corticospinal tract within the tumor-affected hemispheres were performed. The functional motor cortex was enclosed by navigated transcranial magnetic stimulation motor mapping before tumor resection and used for seeding. A range of angular deviation and fractional anisotropy thresholds (for DTI) was tested.

RESULTS: For all investigated thresholds, multilevel fiber tractography achieved the highest mean coverage of the motor maps (eg, angular threshold = 60°; multilevel/constrained spherical deconvolution/DTI, 25% anisotropy threshold = 71.8%, 22.6%, and 11.7%) and the most extensive corticospinal tract reconstructions (eg, angular threshold = 60°; multilevel/constrained spherical deconvolution/DTI, 25% anisotropy threshold = 26,485 mm^3, 6308 mm^3, and 4270 mm^3).

CONCLUSIONS: Multilevel fiber tractography may improve the coverage of the motor cortex by corticospinal tract fibers compared with conventional deterministic algorithms. Thus, it could provide a more detailed and complete visualization of corticospinal tract architecture, particularly by visualizing fiber trajectories with acute angles that might be of high relevance in patients with gliomas and distorted anatomy.

ABBREVIATIONS: ADT = angular deviation threshold; CSD = constrained spherical deconvolution; CST = corticospinal tract; FAT = fractional anisotropy threshold; FOD = fiber orientation distribution; MLFT = multilevel fiber tractography; nTMS = navigated transcranial magnetic stimulation

Gliomas are the most prevalent malignant brain tumors in adults, and particularly anaplastic astrocytoma and glioblastoma as representatives of high-grade gliomas have poor prognoses.[1-3] Contemporary treatment combines neurosurgical tumor resection with extended focal radiation therapy and adjuvant chemotherapy.[4-6] Specifically, a maximum extent of resection correlates to

Received May 15, 2022; accepted after revision January 17, 2023.

From the Department of Biomedical Engineering (A.Z., J.P.), Eindhoven University of Technology, Eindhoven, The Netherlands; Department of Diagnostic and Interventional Radiology (N.S.), University Hospital Ulm, Ulm, Germany; Helmholtz AI (F.K.), Helmholtz Zentrum Munich, Munich, Germany; Department of Diagnostic and Interventional Neuroradiology (N.S., F.K., B.W., C.Z., J.S.K.), School of Medicine, Klinikum rechts der Isar, TUM- Neuroimaging Center (N.S., C.Z., J.S.K., S.M.K.), Klinikum rechts der Isar, Image-Based Biomedical Modeling (F.K., B.M.), Department of Informatics, TranslaTUM (F.K., B.W.), Central Institute for Translational Cancer Research, and Department of Neurosurgery (J.G., A.S., S.M.K.), School of Medicine, Klinikum rechts der Isar, Technical University of Munich, Munich, Germany; Department of Radiology and Biomedical Imaging (N.S.), University of California, San Francisco, San Francisco, California; Department of Imaging and Pathology (A.R., S.S.), Translational MRI, and Department of Neurosciences (A.R., S.S.), Leuven Brain Institute, Katholieke Universiteit Leuven, Leuven, Belgium; Image Sciences Institute (A.D.L., A.L.) and Neurology Department (A.D.L.), University Medical Center Utrecht Brain Center, University Medical Center Utrecht, Utrecht, The Netherlands; and Department of Quantitative Biomedicine (B.M.), University of Zurich, Zurich, Switzerland.

A. Zhylka and N. Sollmann have contributed equally to this work and share the first authorship.

Andrey Zhylka received funding from the European Union's Horizon 2020 research and innovation program under the Marie Sklodowska-Curie grant agreement No. 765148. Bjoern Menze, Benedikt Wiestler, and Florian Kofler are supported through the SFB 824, subproject B12, supported by Deutsche Forschungsgemeinschaft through Technical University of Munich International Graduate School of Science and Engineering, GSC 81.

Please address correspondence to Andrey Zhylka, MD, Eindhoven University of Technology, Biomedical Engineering, Rondom 70, Eindhoven, 5612AP, Netherlands; e-mail: a.zhylka@tue.nl; @AnjensonZ; @NSollmann

Indicates open access to non-subscribers at www.ajnr.org

Indicates article with online supplemental data.

http://dx.doi.org/10.3174/ajnr.A7793

Copyright 2023 by American Society of Neuroradiology.

prolonged survival and improved quality of life.[7-9] However, a maximum extent of resection needs to be weighed against the risk of surgery-related functional decline such as persistent paresis or aphasia, which may arise from tumor resection in or near functionally eloquent structures such as the motor or language cortex.[10,11] Additionally, subcortical WM pathways such as efferent fibers that interconnect certain brain areas or course down to the periphery may need to be respected to avoid lasting functional deficits.[12,13]

Imaging and mapping of brain function are essential for a maximum safe resection combined with a high extent of resection and a low-risk profile for permanent functional deterioration.[6,14-16] In the preoperative setup, DWI with tractography is used for delineation of WM architecture, which can then be visualized and respected during tumor resection.[17,18] Particularly, DTI-based tractography is commonly applied to reconstruct certain fiber tracts, relating to its comparatively wide availability and low false-positive rate.[19] However, despite its frequent application in the preoperative work-up of patients with glioma, the technique has relevant shortcomings that render the accuracy of the method questionable.[20,21] Specifically, major issues relate to potential underrepresentation of fiber branching or crossing fibers, which are difficult to resolve by DTI-based tractography.[22-24] Alternatives to DTI-based tractography exist, including methods such as constrained spherical deconvolution (CSD)—tractography, which has shown improved specificity compared with DTI-based tractography, given that CSD-based tractography is determined by higher angular resolution and the possibility of also disentangling more complex fiber configurations.[25,26] In CSD, multiple fibers passing through a voxel with distinct orientations can be estimated, depending on the fiber orientation distribution (FOD).[25,26]

Multilevel fiber tractography (MLFT) has been developed from CSD-based tractography and similarly propagates fiber pathways on the basis of FOD peaks, with the main advancement that MLFT proposes that FOD peaks do not solely reflect crossing fibers but may also reflect high angular deviation of fibers or their branching.[27,28] A previous study has demonstrated that MLFT improved reconstruction of the corticospinal tract (CST) in patients with motor-eloquent high-grade gliomas by generating fiber bundles with higher radial extent (ie, delineation of CST fanning with a wider range) compared with DTI as well as CSD-based deterministic CST tractography, thus potentially showing a more complete picture of the actual CST architecture.[27] Yet, without optimal seeding of the ROI for tractography, MLFT would be at considerable risk of reconstructing false-positive WM pathways, given that it can also include acute angles of fiber courses, which might be particularly frequently observed among patients with brain tumors due to the space-occupying effect that may lead to fiber diversion and compression.[27]

The issue of optimal ROI seeding for CST reconstruction may be addressed by combining MLFT with preoperative functional mapping, such as navigated transcranial magnetic stimulation (nTMS). In essence, nTMS can target neurostimulation to the brain with subcentimeter precision and enables the spatial identification and demarcation of the motor cortex in relation to a lesion.[29,30] Particularly, nTMS-based motor mapping has been frequently used in the preoperative setup and for guidance of intraoperative resection in patients with motor-eloquent brain tumors.[30-32] The approach has been shown to result in cortical motor maps similar to those generated by intraoperative direct electrical stimulation as the reference standard for functional cortical mapping.[33-35] More recently, combinations of tractography with nTMS have been used to establish function-based tractography of the CST, which is based on the definition of the nTMS-derived cortical motor map as an ROI.[36-40]

Against this background, the purpose of the present study was to combine MLFT for reconstruction of the CST with nTMS for enclosing the functional motor cortex in patients with motor-eloquent gliomas. We hypothesized that MLFT may show higher coverage of the nTMS motor map (ie, the highest percentage of fibers of the CST being connected to the motor cortex) compared with deterministic DTI-based and CSD-based tractography.

MATERIALS AND METHODS

Study Design and Patient Cohort

This study was approved by the local institutional review board (Ethikkommission Technische Universität München) and was conducted in accordance with the Declaration of Helsinki. The requirement for written informed consent for this study was waived due to the retrospective design.

Eligible patients were identified by chart review, covering the time interval from February 2019 to February 2020. Inclusion criteria were the following: 1) older than 18 years of age, 2) availability of preoperative 3T MR imaging, including diffusion-weighted sequences, 3) diagnosis of a high-grade glioma (based on imaging findings and later confirmation by histopathologic evaluation of biopsy probes or tumor tissue harvested during surgical resection), 4) suspected motor-eloquent tumor location according to preoperative MR imaging, and 5) availability of preoperative nTMS-based motor mapping of the tumor-affected hemisphere.

Overall, 31 patients (mean age, 61.5 [SD, 12.2] years; age range, 34.4–85.1 years; 12 women) matched the inclusion criteria and were considered for this study. Three patients were diagnosed with World Health Organization grade III gliomas, and 28 patients with World Health Organization grade IV gliomas, and the right hemisphere was affected by the tumor volume in 19 patients.

Data Acquisition

MR Imaging. Preoperative MR imaging was performed on two 3T scanners (Achieva dStream or Ingenia; Philips Healthcare) using a 32-channel head coil. The imaging protocol included a 3D FLAIR sequence (TR/TE = 4800/277 ms, 1-mm^3 isotropic voxels covering the whole head), an axial T2-weighted sequence (TR/TE = 3396/87 ms, voxel size = 0.36 × 0.36 × 4 mm^3), a diffusion-weighted sequence (TR/TE = 5000/78 ms, voxel size = 2 × 2 × 2 mm^3, 1 volume at b=0 s/mm^2, 32 volumes at b=1000 s/mm^2), and a 3D T1-weighted turbo field echo sequence (TR/TE = 9/4 ms, 1-mm^3 isotropic voxels covering the whole head) without and with intravenous injection of a contrast agent using a dose of 0.2 mL per kg body weight of gadoteric acid (Dotagraf, 0.5 mmol/mL; Jenapharm).

nTMS. Preoperative motor mapping of the tumor-affected hemisphere was performed using nTMS (NBS system 4.3 or 5.0; Nexstim). For neuronavigation, the preoperatively acquired

contrast-enhanced 3D T1-weighted turbo field echo sequence was used. Motor mapping was performed according to a standardized protocol using a figure-of-eight stimulation coil and a biphasic pulse wave application.[30,41] Both representations of upper and lower extremity muscles were mapped within the tumor-affected hemisphere using an intensity of 105%–110% of the individual resting motor threshold for the upper extremity and an intensity of at least 130% of the resting motor threshold for the lower extremity muscles.[30,41] Motor-positive nTMS points were identified during post hoc analysis, which were required to show an amplitude of motor-evoked potentials of $\geq 50\,\mu V$, with motor-evoked potential onset latencies within the typical ranges.[30,42,43]

Image Segmentation and Processing of DWI Data. Before image segmentation, all MR imaging data were transferred to Montreal Neurological Institute space (with an isotropic voxel size of 1 mm^3). Given that commonly used parcellation pipelines may not produce robust segmentations in the presence of brain tumors, lesion filling was performed using the Virtual Brain Grafting toolkit (https://github.com/KUL-Radneuron/KUL_VBG/).[44,45] This approach replaces the tumor volume with synthetic healthy tissue.[45]

As a prerequisite for lesion filling, lesion segmentation was performed using the BraTS toolkit (https://github.com/neuronflow/BraTS-Toolkit).[46,47] The BraTS toolkit was provided with T1-weighted images, both noncontrast and contrast-enhanced, as well as FLAIR and T2-weighted images, to perform the lesion segmentation.[46,47] The segmentation differentiates between the tumor core (necrotic center and contrast-enhancing tumor parts) and FLAIR-hyperintense zones (edema/tumor infiltration).

All diffusion-weighted data sets were preprocessed by performing motion and eddy current corrections.[48] To estimate FODs, we used recursive calibration of the response function.[49] Given the number of acquired diffusion-weighted volumes, the order of spherical harmonics describing FODs was set to $L_{maximum} = 6$. All processing was performed in ExploreDTI (Version 4.8.6; http://www.exploredti.com/).

Because nTMS was performed as a separate acquisition, nTMS points had to be transferred to the space of the T1-weighted and diffusion imaging data sets, achieved by performing registration of the contrast-enhanced T1-weighted images to the masks containing all motor-positive nTMS points of the tumor-affected hemisphere. All nTMS points were enlarged using a hull of 2-mm radius by default to provide the final motor cortex seed mask.[36,37] All image coregistrations and segmentations were visually inspected for quality and manually corrected, when necessary, by a trained neuroradiologist.

Tractography Algorithms. Three tractography algorithms were used for CST reconstruction: DTI-based tractography, CSD-based tractography, and MLFT. MLFT has been recently introduced and is a bundle-specific algorithm that reconstructs fiber bundles as multilevel structures.[27,28] The algorithm requires seed and target regions (ie, the ipsilateral anterior pontine brainstem level and the nTMS-derived cortical motor map) and a maximum number of levels.[27,28] At each iteration, streamline propagation is performed using a deterministic CSD-based algorithm. At the end of each iteration, FOD peaks of the points along pathways that did not reach the target region are used as initial directions at the following iteration. Thus, the potential of the peaks to represent branches is explored.

The angular deviation threshold (ADT) is aimed at maintaining smoothness and physical plausibility of the fiber pathways because it prevents propagation into directions highly deviating from the previous step direction. However, the threshold may impact the accuracy of the reconstruction, depending on the voxel and angular resolution of the data. Thus, each tractography algorithm was run with 3 different ADTs, namely 20°, 45°, and 60°. For DTI-based tractography, 3 levels of the fractional anisotropy threshold (FAT) were used by setting the individual fractional anisotropy to a maximum value that enables reconstructing a minimum fiber course (ie, 100% FAT). For CSD-based tractography as well as MLFT, the FOD peak threshold was set to 0.08.[27,28] The tractography step size was set to half the voxel size, and the number of iterations for MLFT was set to 2.

Statistical Analysis. Statistical testing was performed using SPSS (Version 26.0; SPSS Statistics for Windows; IBM) and the SciPy library (Version 1.3.1; https://www.scipy.org). The threshold for statistical significance was set at $\alpha = .05$.

To assess and compare reconstructions of the CST, we computed the ratio of the visited voxels of the nTMS mask to the reconstructed fibers for each parameter configuration (ADT = 20°, 45°, and 60°; FAT = 25%, 50%, and 75%) and algorithm (DTI-based tractography, CSD-based tractography, and MLFT). This computation provides an estimate of how much of the nTMS mask (ie, cortical motor-positive nTMS points) is covered and, consequently, how complete the reconstruction is according to the function-based reference (nTMS mask). Additionally, volumes of the reconstructed bundles were computed as the accumulated volume of all the voxels visited by at least 1 fiber pathway. Only the bundle part between the seed and target region was taken into account. To compare the nTMS coverage as well as the volumes of the reconstructions as obtained by the different algorithms depending on the FAT as well as ADT, we performed paired 1-sided Wilcoxon tests. Furthermore, the nTMS coverage achieved by the same algorithm at different ADT settings was compared using paired 2-sided Wilcoxon tests.

RESULTS

Tractography using MLFT was capable of reconstructing fiber bundles with higher volumes (on average 10,367, 19,567, and 26,485 mm^3 for ADTs of 20°, 45°, and 60°) than what was achieved by the DTI- and CSD-based algorithms, true for all used ADTs and FATs (Fig 1 and Online Supplemental Data). DTI-based tractography reconstructed statistically significant smaller bundles than CSD-based tractography at 25% ($P = .54$, .99, and 1 for 20°, 45°, and 60° ADT), 50% ($P = .97$, 1, and 1 for 20°, 45°, and 60° ADT) and 75% FAT ($P = 1$ for all ADTs) based on 1-sided Wilcoxon tests.

Compared with the other approaches, MLFT reconstructions of the CST achieved the highest coverage of the nTMS motor map, which amounted to 38.7%, 60.8%, and 71.8%, on average, for ADTs of 20°, 45°, and 60°, respectively (Fig 2 and Online Supplemental Data). MLFT also achieved higher coverage in

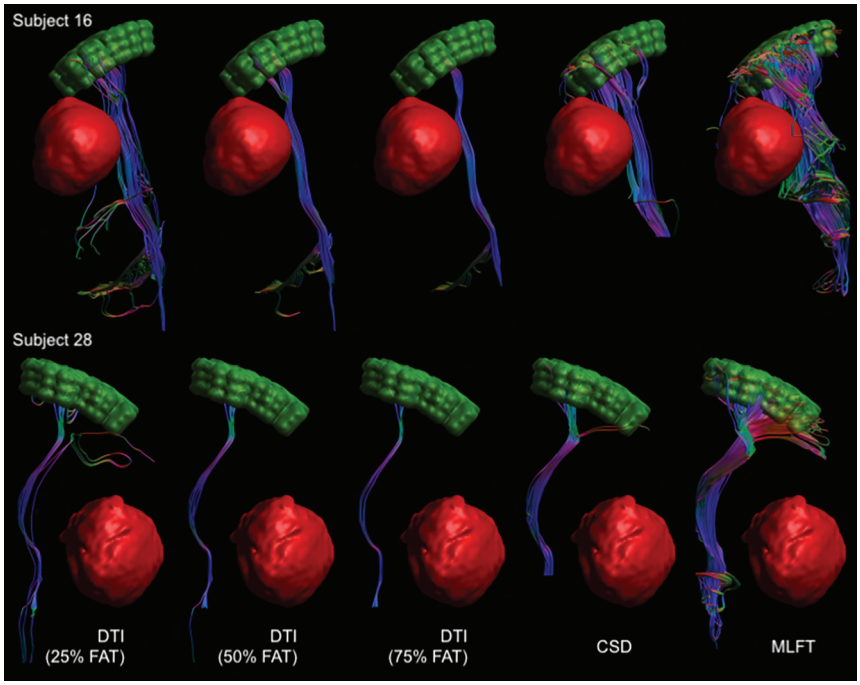

FIG 1. The nTMS-based motor map (green indicates single motor-positive nTMS points with a 2-mm hull) was used as the target region for reconstruction of the CST within the tumor-affected hemisphere (red indicates the tumor core). MLFT shows higher nTMS mask coverage compared with DTI- and CSD-based results, including cases of tumor-induced bundle deformation (subject No. 28).

case of tumor-induced bundle deformations (Fig 1). CSD-based tractography achieved higher coverage of the nTMS motor map than DTI-based tractography, regardless of the settings for ADT and FAT (Fig 2). This finding was also confirmed by comparing reconstructions obtained with the same ADTs with 1-sided Wilcoxon tests ($P > .95$ for all comparisons, Online Supplemental Data).

The change of the ADT led to statistically significant changes in nTMS motor map coverage ($P < .01$) based on 2-sided Wilcoxon tests, which can also be observed in an exemplary patient case (Fig 3). Only when using 75% FAT for DTI-based reconstruction was a statistically nonsignificant difference observed between reconstructions obtained with 20° and 60° ADT as well as 45° and 60° ADT.

DISCUSSION

We combined MLFT with motor mapping for CST reconstruction based on nTMS motor maps used for ROI placement in patients with motor-eloquent gliomas. Tractography results were compared against deterministic DTI-based and CSD-based tractography, given that these techniques are commonly used for clinical tractography in patients with brain tumors. The main findings are as follows: 1) MLFT enabled CST reconstruction with higher bundle volumes, and 2) MLFT yielded higher coverage of the nTMS motor map (ie, a higher percentage of the nTMS points reached by the reconstructed CST).

The MLFT algorithm we used was developed from CSD-based tractography, and it similarly reconstructs fiber pathways on the basis of FOD peaks.[27,28] However, in contrast to CSD-based tractography, MLFT suggests that FOD peaks may also be reflective of high angular deviation of fibers or their branching and may not only stem from fiber crossings.[27,28] Hence, reconstruction of the CST with MLFT may produce bundles with higher radial extent; thus, the delineation of CST fanning with a wider range by also reconstructing fiber courses with acute angles becomes possible.[27,28] Zhylka et al[27] have shown this feature in a previous study among patients with motor-eloquent high-grade gliomas, but the motor cortex mask was defined using a parcellation mask of the precentral, postcentral, and paracentral gyri combined with a cross-section of the brainstem at the pontine level.

Given that MLFT may naturally reconstruct bundles with higher fiber count due to inclusion of fibers that course with acute angles, the potential risk of increasing the false-positive rate (ie, proportion of fibers that are visualized but do not connect to the actual functional motor cortex) is present. Specifically, to avoid a high false-positive rate, MLFT would require well-defined ROI seeding, and if certain pathways do not connect to the ROI, the algorithm checks to see if any deviation at the previous reconstruction points would allow connection to the ROI, thus providing some control over specificity while potentially improving sensitivity.[27,28] In this regard, motor maps from preoperative nTMS were used as the target ROIs, given that nTMS motor mapping has shown high agreement with intraoperative direct electrical stimulation as the reference standard for functional mapping in patients with brain tumor.[33-35] Furthermore, nTMS has also been effectively combined with DTI-based tractography in the past, allowing DTI-based reconstruction of the CST using functional data for ROI seeding, which could improve tracking of fibers for preparation and guidance of tumor resection and stratification for perioperative functional deficits.[36-39,50] In this context, compared with conventional seeding without functional data (eg, manual delineation of the brainstem for ROI generation), nTMS-based tractography of the CST has been shown to result in a lower number of aberrant tracts (ie, tracts not belonging to the CST), and it changed the surgical strategy in more than twice as many patients.[38,50] Furthermore, detailed somatotopic CST reconstructions might become possible when using nTMS motor maps as ROIs, with greater spatial overlap between the motor cortex and the cortical end region of the CST compared with conventional anatomic seeding for tractography.[40]

Reconstructions of the CST using MLFT showed the highest bundle volume for the CST, combined with the highest coverage of the nTMS motor map compared with deterministic DTI- or

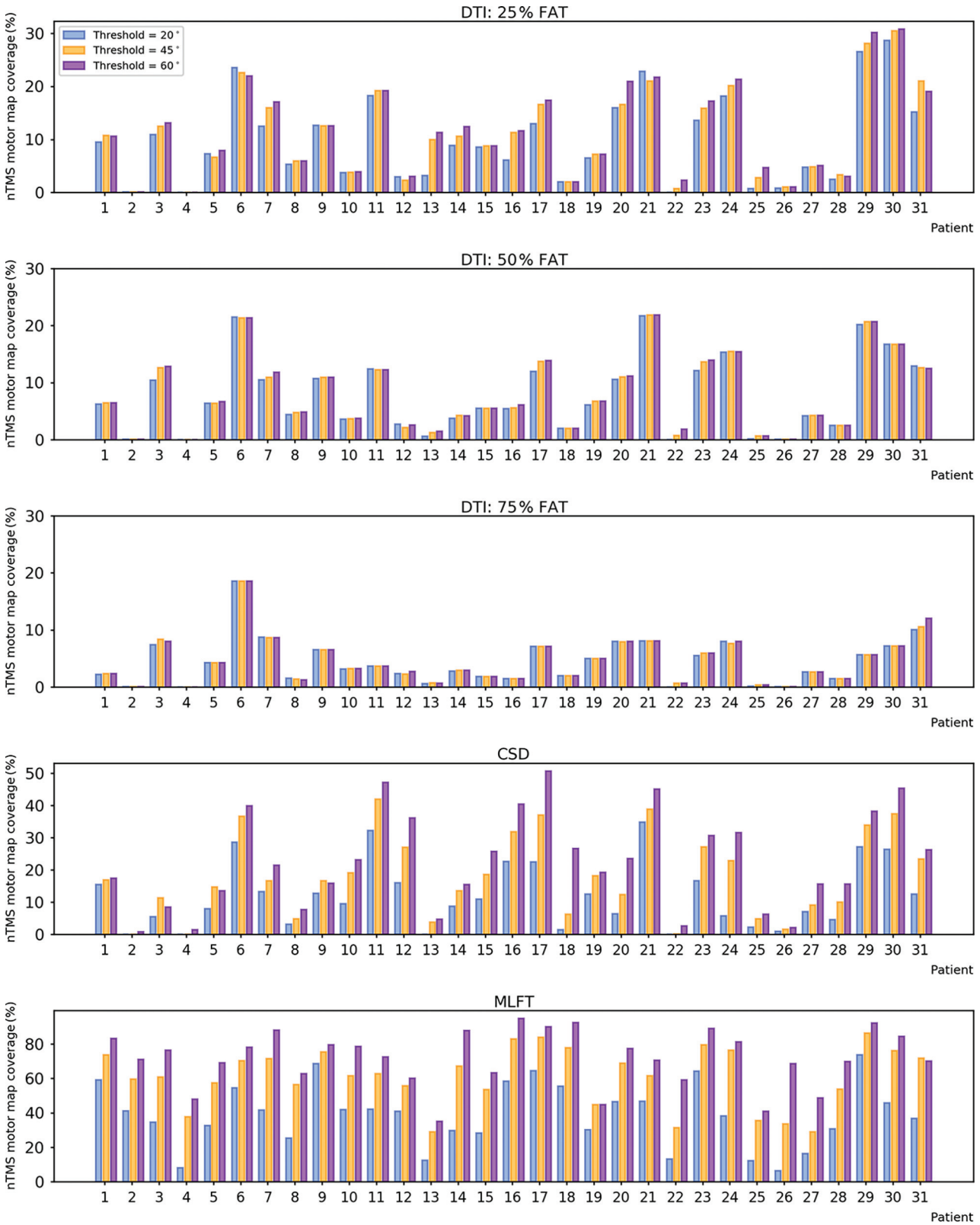

FIG 2. nTMS motor map coverage derived from CST reconstructed with DTI-based (with 25%, 50%, and 75% of the individual FAT), CSD-based, and MLFT tractography. Changes of ADTs appear to only have visible effect on the result of CSD-based tractography and MLFT.

CSD-based tractography. This result may indicate that a more complete reconstruction of the CST can be achieved with MLFT, which is most likely due to reconstruction of fibers with higher radial extents. Glioma may cause considerable deviation of CST fibers, which may, in part, be lost to reconstruction when using DTI- or CSD-based approaches (Fig 1). The higher coverage of nTMS maps when applying MLFT could increase confidence because the fibers reconstructed from MLFT are actually

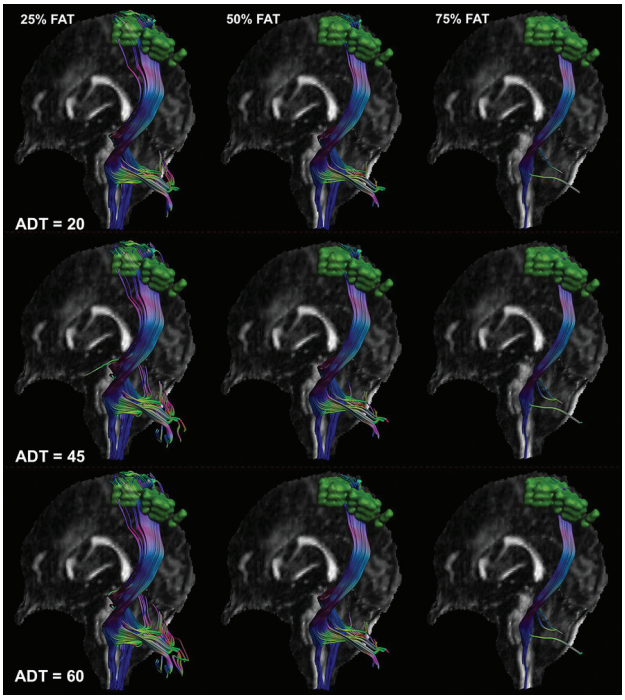

FIG 3. DTI-based reconstructions of the CST with the nTMS-based motor map (green indicates single motor-positive nTMS points with a 2-mm hull) with varied ADT (*rows*) and FAT levels in subject No. 30.

representative of the motor system (Fig 2), given that higher nTMS coverage is suggestive of more fibers being connected to the actual functional motor cortex. Of note, preoperatively enclosing the functional motor cortex with nTMS allows definition of its individual extent and location, which can be drastically aberrant to the structural landmark anatomy due to shifts related to the space-occupying effects and, most notably, due to plastic reshaping of functional motor representations in response to the presence and growth of glioma.[51-53]

A more complete reconstruction of fibers belonging to the CST is of clinical merit when achieving an optimal onco-functional balance because their visualization could help avoid surgery-induced damage and, thus, occurrence of lasting perioperative paresis. Specifically, CST reconstruction with broader fanning by MLFT could also generate laterally coursing and marginal fibers, which could be at particular risk of damage when approaching a maximized extent of resection. The higher CST bundle volumes may likely also result in pathways with a smaller lesion-to-tract distance, having potential impact on resection planning. Previous work using nTMS motor mapping combined with DTI-based tractography of the CST has proposed the lesion-to-tract distance as a parameter for presurgical stratification of the risk of permanent motor function decline, with lower lesion-to-tract distances being associated with a higher risk for lasting deficits.[36,37,39] Application of MLFT instead of DTI-based tracking might potentially allow refined results for lesion-to-tract distances, with a potential definition of more realistic lesion-to-tract distances that may facilitate improved surgical outcome in terms of the extent of resection and the patient's functional status.

A major limitation of this study is that tractography results were not confirmed by intraoperative direct electrical stimulation as the reference standard for functional mapping. Due to the retrospective character of this study, this confirmation was not possible but may be achieved in future studies. Hence, potential overrepresentations of fibers when using the MLFT algorithm cannot be fully excluded. Another limitation of MLFT relates to FOD accuracy, given that a high number of diffusion directions and high b-values are not routinely acquired for clinically used diffusion-weighted MR imaging sequences. As a consequence, the accuracy of the fitted diffusion models could be restricted because FODs have to be represented by lower-order spherical harmonics. Furthermore, the FOD algorithm used does not estimate separate response functions for different tissues.[49] However, using acquisitions with multiple diffusion-weightings (eg, multishell imaging) over the sequence we used would facilitate applying FOD algorithms that can differentiate multiple tissues.[54]

CONCLUSIONS

Compared with routinely used deterministic DTI-based and CSD-based tractography of the CST, MLFT may enable CST reconstructions with a higher bundle volume paired with higher coverage of the functional motor cortex. Thus, MLFT could provide a more detailed visualization of CST architecture by also visualizing fiber courses with acute angles, which might be of particular relevance in patients with gliomas and distorted anatomy of the motor system. However, prospective confirmation of tractography results from MLFT by intraoperative direct electrical stimulation as the reference standard for functional mapping is required for validation purposes.

Disclosure forms provided by the authors are available with the full text and PDF of this article at www.ajnr.org.

REFERENCES

1. Ostrom QT, Bauchet L, Davis FG, et al. **The epidemiology of glioma in adults: a state of the science review.** *Neuro Oncol* 2014;16:896–913 CrossRef Medline
2. Ostrom QT, Cote DJ, Ascha M, et al. **Adult glioma incidence and survival by race or ethnicity in the United States from 2000 to 2014.** *JAMA Oncol* 2018;4:1254–62 CrossRef Medline
3. Miller KD, Ostrom QT, Kruchko C, et al. **Brain and other central nervous system tumor statistics, 2021.** *CA Cancer J Clin* 2021;71:381–406 CrossRef Medline
4. Stupp R, Mason WP, van den Bent MJ; et al; National Cancer Institute of Canada Clinical Trials Group. **Radiotherapy plus concomitant and adjuvant temozolomide for glioblastoma.** *N Engl J Med* 2005;352:987–96 CrossRef Medline
5. Martínez-Garcia M, Álvarez-Linera J, Carrato C, et al. **SEOM clinical guidelines for diagnosis and treatment of glioblastoma (2017).** *Clin Transl Oncol* 2018;20:22–28 CrossRef Medline
6. Sanai N, Berger MS. **Surgical oncology for gliomas: the state of the art.** *Nat Rev Clin Oncol* 2018;15:112–25 CrossRef Medline
7. Lacroix M, Abi-Said D, Fourney DR, et al. **A multivariate analysis of 416 patients with glioblastoma multiforme: prognosis, extent of resection, and survival.** *J Neurosurg* 2001;95:190–98 CrossRef Medline
8. Brown PD, Maurer MJ, Rummans TA, et al. **A prospective study of quality of life in adults with newly diagnosed high-grade gliomas: the impact of the extent of resection on quality of life and survival.** *Neurosurgery* 2005;57:495–503 CrossRef Medline

9. Molinaro AM, Hervey-Jumper S, Morshed RA, et al. **Association of maximal extent of resection of contrast-enhanced and non-contrast-enhanced tumor with survival within molecular subgroups of patients with newly diagnosed glioblastoma.** *JAMA Oncol* 2020;6:495–503 CrossRef Medline
10. Duffau H, Mandonnet E. **The "onco-functional balance" in surgery for diffuse low-grade glioma: Integrating the extent of resection with quality of life.** *Acta Neurochir (Wien)* 2013;155:951–57 CrossRef Medline
11. Bush NAO, Chang SM, Berger MS. **Current and future strategies for treatment of glioma.** *Neurosurg Rev* 2017;40:1–14 CrossRef Medline
12. Stadlbauer A, Nimsky C, Buslei R, et al. **Diffusion tensor imaging and optimized fiber tracking in glioma patients: histopathologic evaluation of tumor-invaded white matter structures.** *Neuroimage* 2007;34:949–56 CrossRef Medline
13. Bello L, Gambini A, Castellano A, et al. **Motor and language DTI fiber tracking combined with intraoperative subcortical mapping for surgical removal of gliomas.** *Neuroimage* 2008;39:369–82 CrossRef Medline
14. Hervey-Jumper SL, Berger MS. **Maximizing safe resection of low- and high-grade glioma.** *J Neurooncol* 2016;130:269–82 CrossRef Medline
15. Villanueva-Meyer JE, Mabray MC, Cha S. **Current clinical brain tumor imaging.** *Clin Neurosurg* 2017;81:397–415 CrossRef Medline
16. Carrete LR, Young JS, Cha S. **Advanced imaging techniques for newly diagnosed and recurrent gliomas.** *Front Neurosci* 2022;16:787755 CrossRef Medline
17. Henderson F, Abdullah KG, Verma R, et al. **Tractography and the connectome in neurosurgical treatment of gliomas: the premise, the progress, and the potential.** *Neurosurg Focus* 2020;48:E6 CrossRef Medline
18. Yeh FC, Irimia A, de Almeida Bastos DC, et al. **Tractography methods and findings in brain tumors and traumatic brain injury.** *Neuroimage* 2021;245:118651 CrossRef Medline
19. Maier-Hein KH, Neher PF, Houde JC, et al. **The challenge of mapping the human connectome based on diffusion tractography.** *Nat Commun* 2017;8:1349 CrossRef Medline
20. Duffau H. **Diffusion tensor imaging is a research and educational tool, but not yet a clinical tool.** *World Neurosurg* 2014;82:e43–45 CrossRef
21. Azad TD, Duffau H. **Limitations of functional neuroimaging for patient selection and surgical planning in glioma surgery.** *Neurosurg Focus* 2020;48:E12 CrossRef Medline
22. Behrens TE, Berg HJ, Jbabdi S, et al. **Probabilistic diffusion tractography with multiple fibre orientations: what can we gain?** *Neuroimage* 2007;34:144–55 CrossRef Medline
23. Farquharson S, Tournier JD, Calamante F, et al. **White matter fiber tractography: why we need to move beyond DTI.** *J Neurosurg* 2013;118:1367–77 CrossRef Medline
24. Jeurissen B, Leemans A, Tournier JD, et al. **Investigating the prevalence of complex fiber configurations in white matter tissue with diffusion magnetic resonance imaging.** *Hum Brain Mapp* 2013;34:2747–66 CrossRef Medline
25. Tournier JD, Calamante F, Connelly A. **Robust determination of the fibre orientation distribution in diffusion MRI: non-negativity constrained super-resolved spherical deconvolution.** *Neuroimage* 2007;35:1459–72 CrossRef Medline
26. Jeurissen B, Leemans A, Jones DK, et al. **Probabilistic fiber tracking using the residual bootstrap with constrained spherical deconvolution.** *Hum Brain Mapp* 2011;32:461–79 CrossRef Medline
27. Zhylka A, Sollmann N, Kofler F, et al. **Tracking the corticospinal tract in patients with high-grade glioma: clinical evaluation of multi-level fiber tracking and comparison to conventional deterministic approaches.** *Front Oncol* 2021;11:761169 CrossRef Medline
28. Zhylka A, Leemans A, Pluim JP, et al. **Anatomically informed multi-level fiber tractography for targeted virtual dissection.** *Magn Reson Mater Phy* 2022 Jul 29. [Epub ahead of print] CrossRef Medline
29. Ruohonen J, Karhu J. **Navigated transcranial magnetic stimulation.** *Neurophysiol Clin* 2010;40:7–17 CrossRef Medline
30. Sollmann N, Krieg SM, Säisänen L, et al. **Mapping of motor function with neuronavigated transcranial magnetic stimulation: a review on clinical application in brain tumors and methods for ensuring feasible accuracy.** *Brain Sci* 2021;11:897 CrossRef Medline
31. Lefaucheur JP, Picht T. **The value of preoperative functional cortical mapping using navigated TMS.** *Neurophysiol Clin* 2016;46:125–33 CrossRef Medline
32. Haddad AF, Young JS, Berger MS, et al. **Preoperative applications of navigated transcranial magnetic stimulation.** *Front Neurol* 2021;11:628903 CrossRef Medline
33. Forster MT, Hattingen E, Senft C, et al. **Navigated transcranial magnetic stimulation and functional magnetic resonance imaging: advanced adjuncts in preoperative planning for central region tumors.** *Neurosurgery* 2011;68:1317–24 CrossRef Medline
34. Krieg SM, Shiban E, Buchmann N, et al. **Utility of presurgical navigated transcranial magnetic brain stimulation for the resection of tumors in eloquent motor areas: clinical article.** *J Neurosurg* 2012;116:994–1001 CrossRef Medline
35. Tarapore PE, Tate MC, Findlay AM, et al. **Preoperative multimodal motor mapping: a comparison of magnetoencephalography imaging, navigated transcranial magnetic stimulation, and direct cortical stimulation: clinical article.** *J Neurosurg* 2012;117:354–62 CrossRef Medline
36. Sollmann N, Wildschuetz N, Kelm A, et al. **Associations between clinical outcome and navigated transcranial magnetic stimulation characteristics in patients with motor-eloquent brain lesions: a combined navigated transcranial magnetic stimulation-diffusion tensor imaging fiber tracking approach.** *J Neurosurg* 2018;128:800–10 CrossRef Medline
37. Sollmann N, Zhang H, Fratini A, et al. **Risk assessment by presurgical tractography using navigated TMS maps in patients with highly motor- or language-eloquent brain tumors.** *Cancers (Basel)* 2020;12:1264 CrossRef Medline
38. Frey D, Strack V, Wiener E, et al. **A new approach for corticospinal tract reconstruction based on navigated transcranial stimulation and standardized fractional anisotropy values.** *Neuroimage* 2012;62:1600–09 CrossRef Medline
39. Rosenstock T, Grittner U, Acker G, et al. **Risk stratification in motor area-related glioma surgery based on navigated transcranial magnetic stimulation data.** *J Neurosurg* 2017;126:1227–37 CrossRef Medline
40. Conti A, Raffa G, Granata F, et al. **Navigated transcranial magnetic stimulation for "somatotopic" tractography of the corticospinal tract.** *Operative Neurosurgery* 2014;10:542–54; discussion 554 CrossRef Medline
41. Krieg SM, Lioumis P, Mäkelä JP, et al. **Protocol for motor and language mapping by navigated TMS in patients and healthy volunteers: workshop report.** *Acta Neurochir (Wien)* 2017;159:1187–95 CrossRef Medline
42. Säisänen L, Julkunen P, Niskanen E, et al. **Motor potentials evoked by navigated transcranial magnetic stimulation in healthy subjects.** *J Clin Neurophysiol* 2008;25:367–72 CrossRef Medline
43. Sollmann N, Bulubas L, Tanigawa N, et al. **The variability of motor evoked potential latencies in neurosurgical motor mapping by preoperative navigated transcranial magnetic stimulation.** *BMC Neurosci* 2017;18:5 CrossRef Medline
44. Fischl B. **FreeSurfer.** *Neuroimage* 2012;62:774–81 CrossRef Medline
45. Radwan AM, Emsell L, Blommaert J, et al. **Virtual brain grafting: enabling whole brain parcellation in the presence of large lesions.** *Neuroimage* 2021;229:117731 CrossRef Medline
46. Menze BH, Jakab A, Bauer S, et al. **The multimodal Brain Tumor Image Segmentation Benchmark (BRATS).** *IEEE Trans Med Imaging* 2015;34:1993–2024 CrossRef Medline
47. Kofler F, Berger C, Waldmannstetter D, et al. **BraTS Toolkit: translating BraTS brain tumor segmentation algorithms into clinical and scientific practice.** *Front Neurosci* 2020;14:125 CrossRef Medline

48. Mohammadi S, Möller HE, Kugel H, et al. **Correcting eddy current and motion effects by affine whole-brain registrations: evaluation of three-dimensional distortions and comparison with slicewise correction.** *Magn Reson Med* 2010;64:1047–56 CrossRef Medline
49. Tax CM, Jeurissen B, Vos SB, et al. **Recursive calibration of the fiber response function for spherical deconvolution of diffusion MRI data.** *Neuroimage* 2014;86:67–80 CrossRef Medline
50. Krieg SM, Buchmann NH, Gempt J, et al. **Diffusion tensor imaging fiber tracking using navigated brain stimulation: a feasibility study.** *Acta Neurochir (Wien)* 2012;154:555–63 CrossRef Medline
51. Southwell DG, Hervey-Jumper SL, Perry DW, et al. **Intraoperative mapping during repeat awake craniotomy reveals the functional plasticity of adult cortex.** *J Neurosurg* 2016;124:1460–69 CrossRef Medline
52. Conway N, Wildschuetz N, Moser T, et al. **Cortical plasticity of motor-eloquent areas measured by navigated transcranial magnetic stimulation in patients with glioma.** *J Neurosurg* 2017;127:981–91 CrossRef Medline
53. Gibb WR, Kong NW, Tate MC. **Direct evidence of plasticity within human primary motor and somatosensory cortices of patients with glioblastoma.** *Neural Plast* 2020;2020:8893708 CrossRef Medline
54. De Luca A, Guo F, Froeling M, et al. **Spherical deconvolution with tissue-specific response functions and multi-shell diffusion MRI to estimate multiple fiber orientation distributions (mFODs).** *Neuroimage* 2020;222:117206 CrossRef Medline